FATIGUE STRESS CONCENTRATION STUDIES ON ALUMINUM ALLOYS

Thesis by

Aram O. Dervishyan

In Partial Fullfillment of the Requirements for the Degree of Aeronautical Engineer

California Institute of Technology

Pasadena, California

1952

ACKNOWLEDGEMENTS

The author wishes to acknowledge the helpful suggestions and efforts in the preparation of this report as follows:

Robert A. Chase, a co-worker on the experimental and theoretical program,

Drs. E. E. Sechler; M. L. Williams; D. E. Hudson for guidance,

Milton Wood for photography,

C. A. Bartsch; William Bowen and GALCIT Machine Shop crew for equipment and repairs,

Betty Wood for presentation of data and

June Royce for typing.

SUMMARY

Fatigue tests in reversed bending were conducted in 75S-T6 and 17S-T6 aluminum alloys to determine whether Neuber's theory on fatigue stress concentration factors in notches was applicable to these materials. The results of the tests indicate confirmation of the theory within engineering accuracy providing the value of ρ' (a material constant) is determined experimentally.

Material size effect was investigated and found to exist. This was an unexpected result since other sources (see References 3 and 4) indicated that no size effect existed for aluminum alloys.

Ignoring the correction due to size effect a value of the Neuber's constant ρ' of approximately 0.05" gave reasonable checks with the experimental data for both 75S-T6 and 17S-T6 aluminum alloys. This may indicate that this value of ρ' is the correct material constant for aluminum alloys but additional data on other alloys is needed to confirm this conclusion.

TABLE OF CONTENTS

I. INTRODUCTION

By the use of the theory of elasticity and the concept of an elementary structural unit of material, Neuber derived the following relation for the fatigue stress concentration factor as applied to the geometrical configuration shown in Fig. 1 (Reference 1):

$$K_f = 1 + \frac{K_t - 1}{1 + \frac{\pi}{\pi - \omega}\sqrt{\frac{\rho'}{\rho}}} \qquad (1)$$

where

K_f = the actual fatigue stress concentration factor

K_t = the geometrical (theoretical) stress concentration factor

ρ' = a material constant which Neuber regarded as the dimension of an elementary unit of material, (in inches)

ρ = the bottom radius of the notch

ω = the angle of the notch wall in radians.

To facilitate the determination of K_t, Neuber established a nomogram from which K_t may be determined from the geometrical parameter of the specimen. This is shown in Fig. 5. One should note that

$$K_t = \frac{\text{maximum longitudinal stress at bottom of notch}}{\text{nominal longitudinal stress from } \sigma = Ma/I}$$

Neuber realized that the actual fatigue stress concentration would be lower than the geometrical stress concentration factor obtained from simple elastic theory. Thus, Eq. (1) contains an empirical constant ρ' which accounts for this difference. In general, must be determined experimentally and this involves the testing of relatively large numbers of specimens in fatigue.

Neuber's theory has been applied to steel specimens where the number of test data is large and where the tests cover many different geometrical configurations. The results show good agreement and indicate that a constant value of ρ' applies for nearly all types of steel alloys. (References 1, 8, and 9).

The purpose of this research program was to study the applicability of Neuber's work to the aluminum alloys as used in the aircraft industry. Accordingly, rotating beam fatigue tests were carried out on notched and unnotched specimens made from 17S-T6 and 75S-T6. These alloys were chosen because they represent one of the older and one of the newer aluminum alloys utilized in airframe manufacture. Semi-circular notches were used and it was assumed that the geometric stress concentration factor for the semi-circular notch was the same as that for a hyperbolic notch having the same bottom radius and depth. (References 8 and 9.)

II. SPECIMENS

All specimens were cut from rolled Alcoa bar stock and conformed to the usual ASTM specimens for use in the R. R. Moore reverse bending fatigue machine. The basic, unnotched specimen had a minimum diameter of 0.300". For the notched specimens, semi-circular notches were cut at the center, these notches having radii of 0.010", 0.015", 0.020", 0.030", and 0.060", (see Plate 1).

For the purpose of investigating size effect, unnotched specimens of 75S-T6, having minimum diameters equal to the diameters of the notched specimens at the bottom of the notches, were tested. The diameters were 0.280", 0.240", and 0.180" respectively. (See Plate 2.) Insufficient time was available to carry out size effect tests on the 17S-T6 alloy.

The surfaces of all specimens were finished to approximately 5 micro-inches by applying in sequence 1) fine emery of 600 grit and 2) levigated alumina applied with oil on a cloth. According to other sources (Reference 7), finishes obtained by the use of 00 or 000 emery cloth would result in negligible improvement in fatigue strength.

III. TEST PROCEDURE

The testing machines used were a bank of four R. R. Moore rotating beam fatigue machines. Since the specimens were small, the tare load of these machines (which was 10 lb.) had to be eliminated. This was done by bolting counterweighted arms to the bearing oil holes (see Plate 4). All tests were carried out at approximately 10,000 rpm.

Since the strength of aluminum alloys decreases rapidly with an increase in temperature (see Fig. 6) an effort was made to provide sufficient ventilation around the specimens and the testing machine so that no appreciable temperature rise above room temperature occurred.

Typical σ_N vs. N curves were obtained for all configurations (Figs. 11-24 inc.). These were carried out to 10^8 cycles and the value of σ_N at 10^8 cycles was taken as the endurance limit.

IV. DATA REDUCTION AND CORRELATION

From the experimental data of σ_N vs. N, average curves were drawn to represent the endurance limit at any number of cycles (see Figs. 11-24 inc.). As in any set of fatigue data there is a reasonable amount of scatter but it should be noticed in the above figures that the scatter has been accentuated by displacing the origin of the σ_N axis. From the average curve, a value of σ_N for $N = 10^8$ cycles has been chosen to represent the endurance limit of each configuration.

From Eq. (1) we see that, when $\omega = 0$

$$K_f = 1 + \frac{K_t - 1}{1 + \sqrt{\frac{\rho'}{\rho}}} \qquad (2)$$

Study of this equation indicates that as $\rho \to 0$ $K_f \to 1$ and as $\rho \to \infty$, $K_f \to K_t = 1$. The nomogram of Fig. 5 indicates that the maximum value of K_t for semi-circular notches ($t/\rho = 1.0$) is 3.0. Hence, K_f will vary with the geometric parameter $\sqrt{\frac{a}{\rho}}$ as shown in Fig. 2. This appears consistent with physical considerations of material behavior under fatigue loading.

Solving Eq. (2) for ρ', we obtain

$$\rho' = \rho \left[\frac{K_t - K_f}{K_f - 1} \right]^2 \qquad (3)$$

and, if there is a definite material factor for aluminum alloys, should be constant. Using the experimental data for the 75S-T6 alloy notched specimens, Table VIII, and an endurance limit of $\sigma_N = 22,000$ psi for the unnotched specimens and we obtain values of ρ' as shown in Table I.

The value of ρ' for ρ = 0.06" is neglected because of the experimental error that is introduced by the fact that differences of large quantities of similar magnitude are squared in calculating ρ' Taking the average of the remaining values of ρ' we get a value of ρ_{AV} of approximately 0.05" for 75S-T6 alloy. It is to be noted that large variations in ρ' result in relatively small variations in the fatigue factor K_f. (See Reference 8.)

Taking an average value of ρ' = 0.05", and computing K_f for the various test specimens, we obtain the results shown in Table II and plotted in Fig. 7. With the exception of the value for ρ = 0.06", the calculated and experimental values of K_f agree within approximately $\pm$ 6 percent.

Another series of smooth specimens having diameters equal to the diameter at the bottom of the notch was then tested to determine if any size effect existed. The σ_N vs. N curves for these specimens are given in Figs. 16-19 inc. and the endurance limit (σ_N at $N = 10^8$ cycles) as a function of size is shown in Table IX and plotted in Fig. 8. If we then use this curve to determine the experimental value of K_f and ρ' we obtain data such as that shown in Table III and plotted in Fig. 9. In this case ρ' = 0.036" and this average value is used to determine K_f (calculated) in Table III and Fig. 9. Even though Fig. 8 appears to give a definite size effect, its introduction into the Neuber equation does not tend to increase the agreement with the experimental data.

The same procedure was used in treating the data for the 17S-T6 specimens. From Table IV the value of the endurance limit for unnotched specimens was taken as σ_N = 20,000 psi. Using this value and the endurance limits for the notched specimens as determined from Figs 21-24 inc. and Table VII, values of ρ' were calculated as shown in Table V. The average value of ρ' from Table V is equal to 0.046" and this has been used to determine K_f (calculated) in Table V and plotted in Fig. 10. As shown, this use of an average value of 0.046" gives agreement in K_f values within $\pm$ 6 percent. If, on the other hand, a value of 0.05" is used for for the 17S-T6 data, the results are as shown in Table VI where again the variation between K_f (calculated) and K_f (experimental) is of the order of 6-7 percent.

Time did not permit an attempt to check size effect on the 17S-T6 specimens. There is, therefore, no correction for size available for this material. According to ANC-5a which refers to basic tests conducted at Alcoa, no appreciable size effect was determined in specimens up to 2" in diameter. (See Reference 6.) From physical considerations, it can be deduced that size effect should act as indicated in Fig. 3. The dotted region is uncertain but it is believed that a maximum value of σ_N will occur for some small size specimens. If size effect were appreciable, neglecting it in applying Neuber's equation, Eq. (2), would lead to non-conservative values of K_f. Although some size effect was noticed in the 75S-T6 specimens (see Fig. 8) it was relatively small and any effect it might have had on K_f was overshadowed by other factors.

V. CONCLUSIONS

The following conclusions were reached as a result of this study:

1. That the Neuber equation for determining the fatigue stress concentration appears to give reasonably accurate results for the two aluminum alloys tested.

2. That an average value of $\rho' = 0.05''$ for the two alloys tested gives values of the fatigue stress concentration factor K_f, which are in reasonably good agreement with the experimental data.

3. That although some size effect was noticed in the 75S-T6 specimens, its effect on the value of K_f or ρ' was overshadowed by other experimental scatter.

The above conclusions are dependent upon the fact that the endurance limit has been defined as that value of σ_N leading to failure at 10^8 stress cycles. Since a complete investigation of size effect was not carried out, the value of ρ' quoted can only be safely used for approximately the size of specimens tested in this program.

VI. RECOMMENDATIONS

Additional fatigue testing should be carried out in the aluminum alloys covering the following items:

1. Alloys other than those tested in this program.

2. A wide range of specimen sizes and notch sizes and shapes.

When sufficient data has been collected on aluminum alloys, an attempt should be made to use statistical analysis methods to more accurately determine the governing parameters of the problem and their influence on the fatigue stress concentration factor.

REFERENCES

1. Neuber, Hans: Kerbspannungrlehre; Published by Edwards Brothers Lts., Ann Arbor, Michigan.

2. ALCOA Structural Handbook - 1951.

3. ANC-5a

4. Hartmann, E. C., Howell, F. M. and Templin, R. L.: How to Use High Strength Aluminum Alloys: ALCOA - Official Report published in Aviation Week, October 10, 1949.

5. ASTM Proc. Vol. 41, Page 133.

6. Moore, H. F., Morkovin, D.: ASTM Proc. Vol. 42, Page 145.

7. Moore, H. F., Morkovin, D.: ASTM Proc. Vol. 44, Page 109.

8. Moore, H. F., Morkovin, D.: ASTM Proc. Vol. 44, Page 137.

9. Moore, H. F., Morkovin, D.: ASTM Proc. Vol. 45, Page 507.

TABLES

I	75ST-6				
ρ	0.01	0.015	0.02	0.03	0.06
$\sqrt{\frac{a}{\rho}}$	3.74	3.00	2.54	2.00	1.23
K_t	2.42	2.19	2.00	1.75	1.33
K_f Exper.	1.38	1.52	1.35	1.41	1.03
ρ'	0.078	0.026	0.067	0.021	6.00

II	75ST-6				
ρ	0.01	0.015	0.02	0.03	0.06
$\sqrt{\frac{a}{\rho}}$	3.74	3.00	2.54	2.00	1.23
K_t	2.42	2.19	2.00	1.75	1.33
K_f Exper.	1.38	1.52	1.35	1.41	1.03
K_f Calcul.	1.44	1.42	1.36	1.33	1.17
% Error	+4.16	-6.60	+.74	-5.70	+13.6

III	75ST-6				
ρ	.01	.015	.02	.03	.06
$\sqrt{\frac{a}{\rho}}$	3.74	3.00	2.54	2.00	1.23
K_t	2.42	2.19	2.00	1.75	1.33
K_f Exper.	1.42	1.58	1.43	1.52	1.16
ρ'	0.057	0.016	0.035	0.0059	0.068
K_f Calcul.	1.49	1.47	1.43	1.36	1.19
% Error	+4.90	-7.00	0.00	-10.5	+2.60

IV	17ST-6	
Specimen Number	Stress lbs/sq.in.	No. of Rev. x 1,000
1	20,000	132,340*
2	20,000	108,880*
3	20,800	113,060*

* No break.

V	17ST-6				
ρ	0.01	0.015	0.02	0.03	0.06
$\sqrt{\frac{a}{\rho}}$	3.74	3.00	2.54	2.00	1.23
K_t	2.42	2.19	2.00	1.75	1.33
K_f Exper.	1.54	1.47	1.40	1.29	1.10
ρ'	0.0266	0.0352	0.045	0.0755	0.317
K_f* Calcul.	1.45	1.43	1.40	1.35	1.18
% Error	-6 percent	-2.7 per-cent	0.00	+4.60 percent	+6.40 percent

* K_f calculated from $\rho' = 0.046''$.

VI	17ST-6				
ρ	0.01	0.015	0.02	0.03	0.06
K_f Calcul.	1.44	1.42	1.39	1.33	1.16
K_f Exper.	1.54	1.47	1.40	1.29	1.10
% Error	-6.50	-3.40	-0.70	+3.00	+4.50

VII — 75ST-6 Notched

ρ	0.010"	0.015"	0.020"	0.030"	0.060"
σ_N lbs./sq. in. At $N=10^8$	13,000	13,640	14,250	15,550	18,200

VIII — Notched 75ST-6

D	0.180"	0.240"	0.260"	0.270"	0.280"
ρ	0.06"	0.03"	0.02"	0.015"	0.010"
σ_N lbs/sq. in. At $N=10^8$	16,000	15,600	16,290	14,530	16,000

IX — Unnotched 75ST-6

D	0.180"	0.240"	0.260"	0.270"	0.280"
σ_N lbs/sq. in. At $N=10^8$	24,600	23,750	23,250	22,950	22,650

(continued)

D	0.300"
σ_N lbs/sq. in. At $N=10^8$	22,000

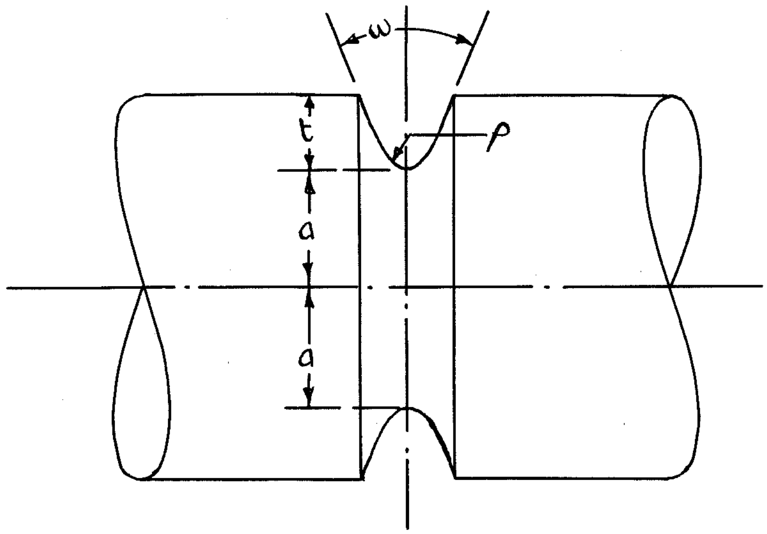

FIG. 1

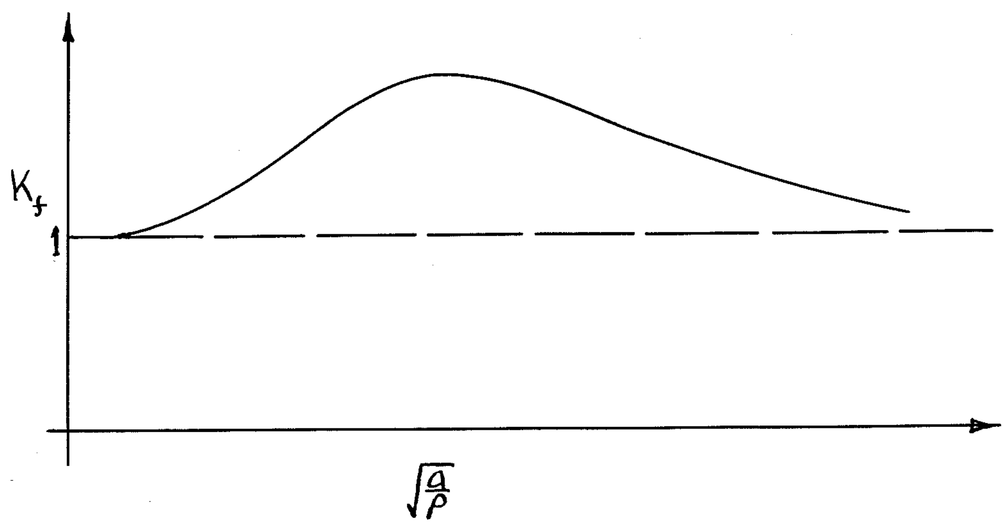

FIG. 2

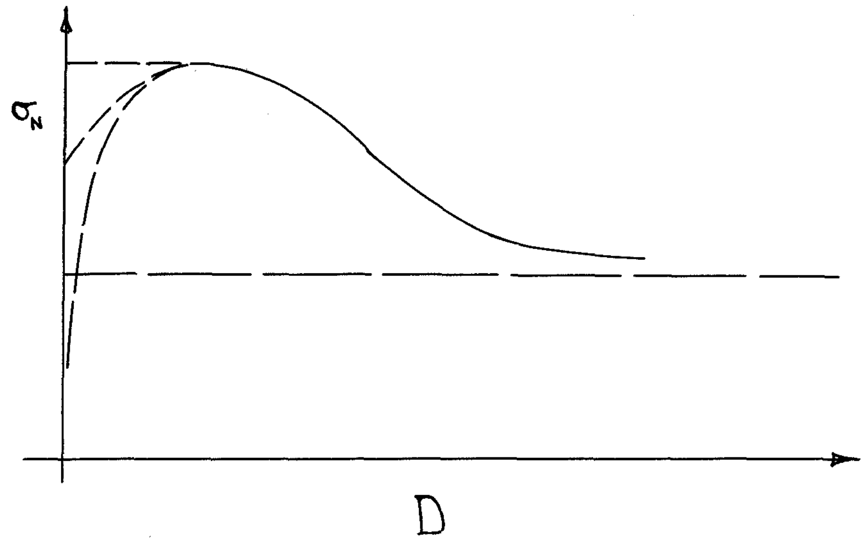

FIG. 3

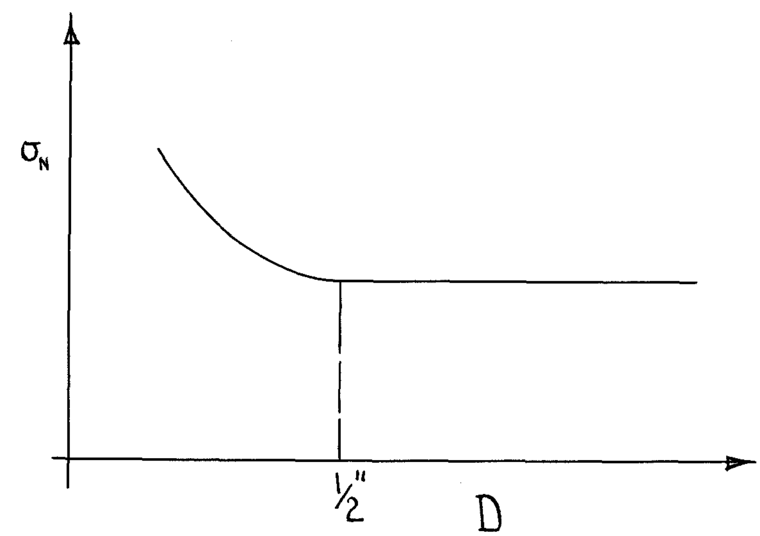

FIG. 4

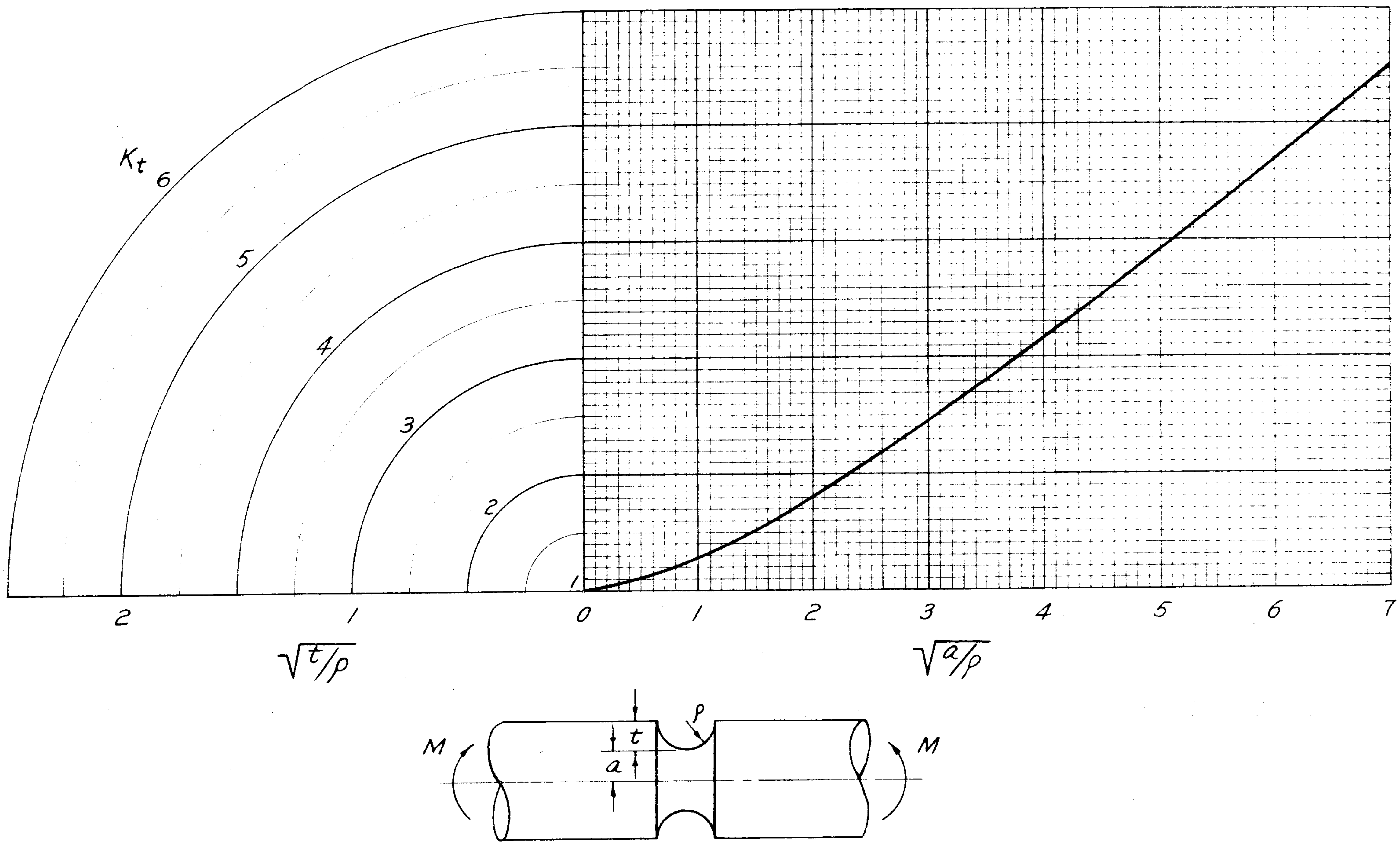

FIG. 5

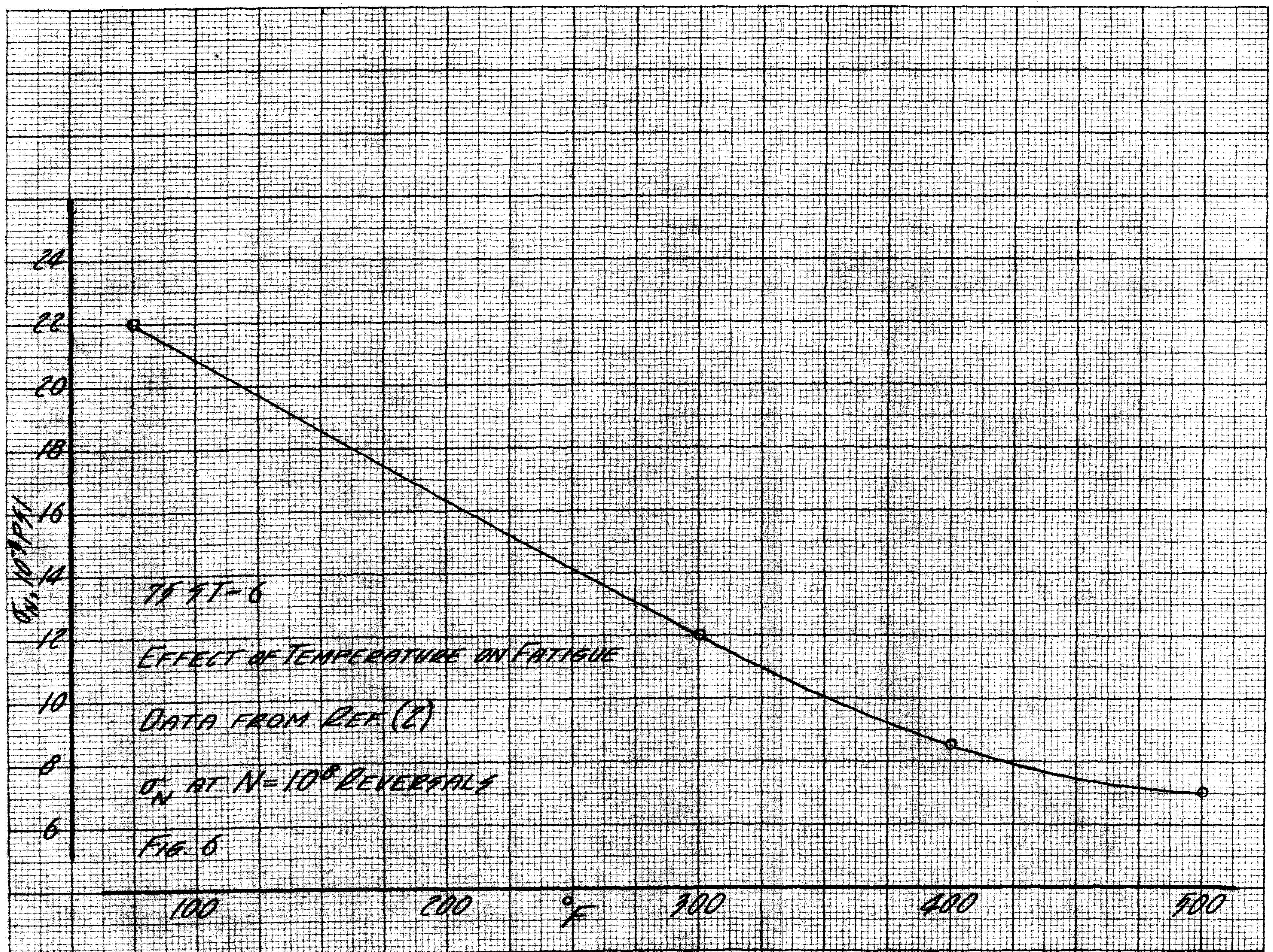
24
22
20
18
16
14
12
10
8
6
σN, 10³ PSI
75 ST-6
EFFECT OF TEMPERATURE ON FATIGUE
DATA FROM REF. (2)
σN AT N=10⁸ REVERSALS
100
200
°F
300
400
500

FIG. 6

CLEARPRINT PAPER CO. T38 20 X 20 DIVISIONS PER INCH 150 X 200 DIVISIONS PRINTED IN U.S.A. ON CLEARPRINT TECHNICAL PAPER NO. 1000H

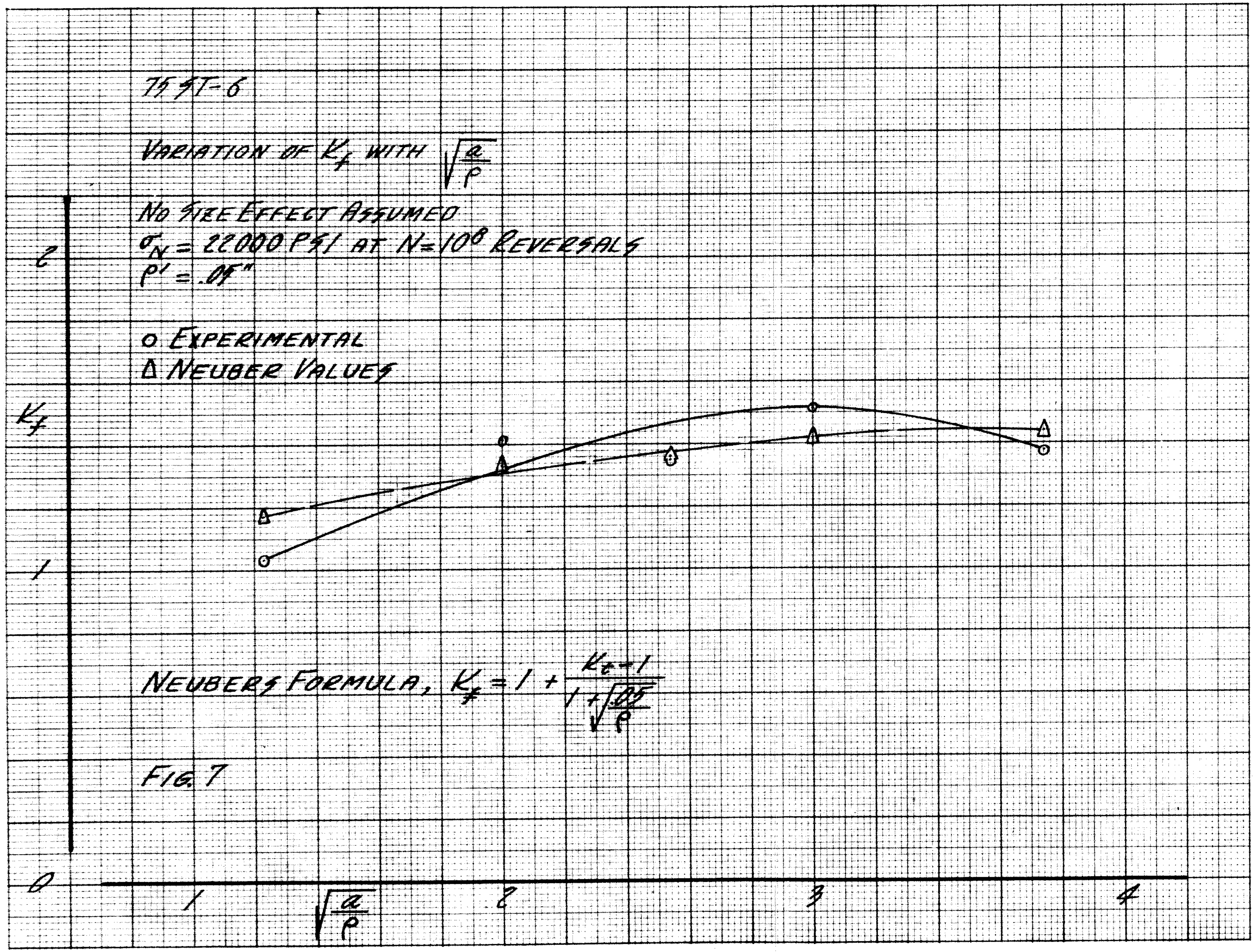

FIG. 7

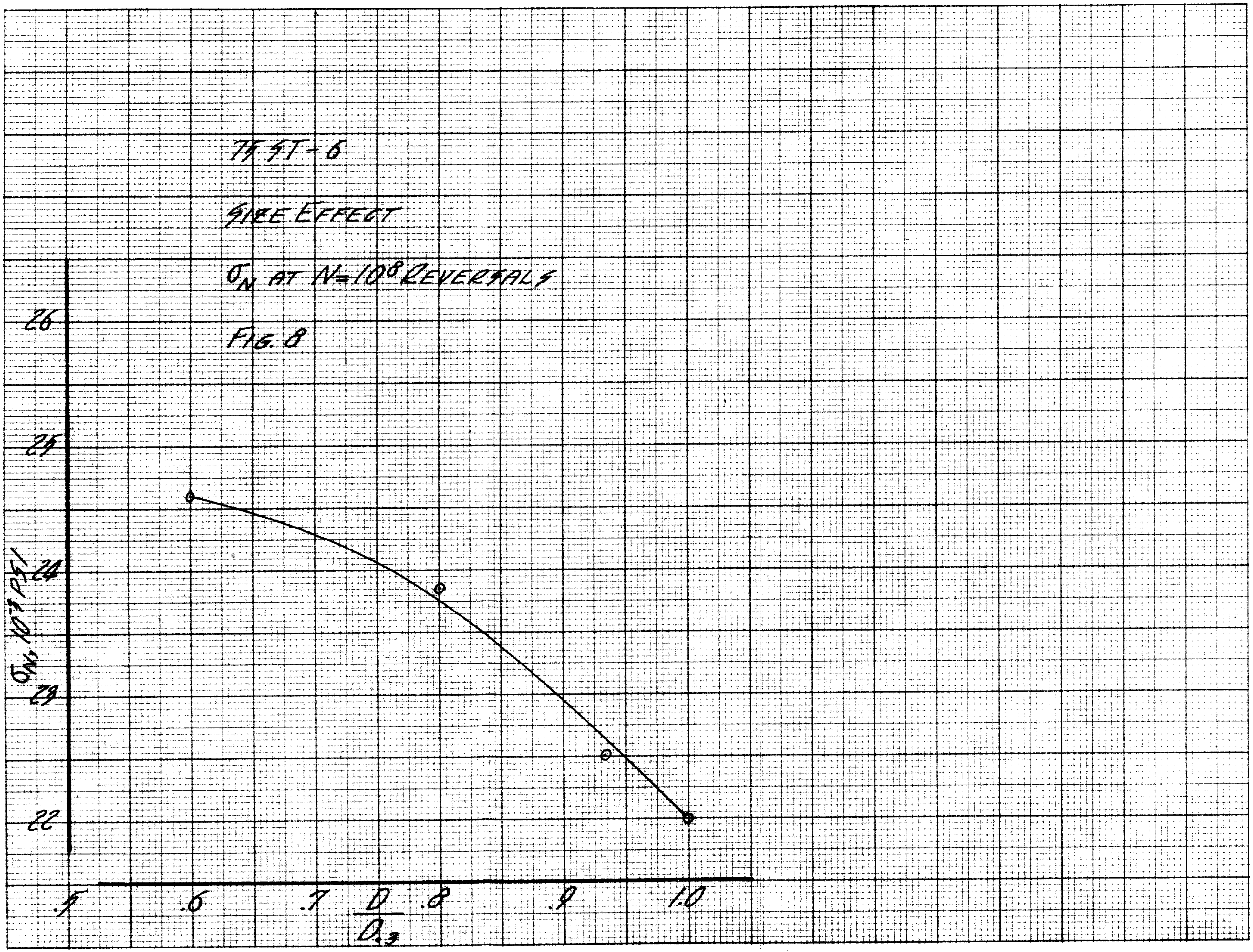
75 ST-6
SIZE EFFECT
σN AT N=10^8 REVERSALS
FIG. 8
26
25
24
23
22
σN, 10^3 PSI
.5
.6
.7
.8
.9
1.0
D/D.3

CLEARPRINT PAPER CO. T38 20 X 20 DIVISIONS PER INCH 150 X 200 DIVISIONS 20 PRINTED IN U.S.A. ON CLEARPRINT TECHNICAL PAPER NO. 1000H

75 ST-6

VARIATION OF K_f WITH $\sqrt{\frac{a}{\rho}}$

SIZE EFFECT TAKEN INTO CONSIDERATION

σ_N PSI AT $N = 10^8$ REVERSALS

$\rho' = .036''$

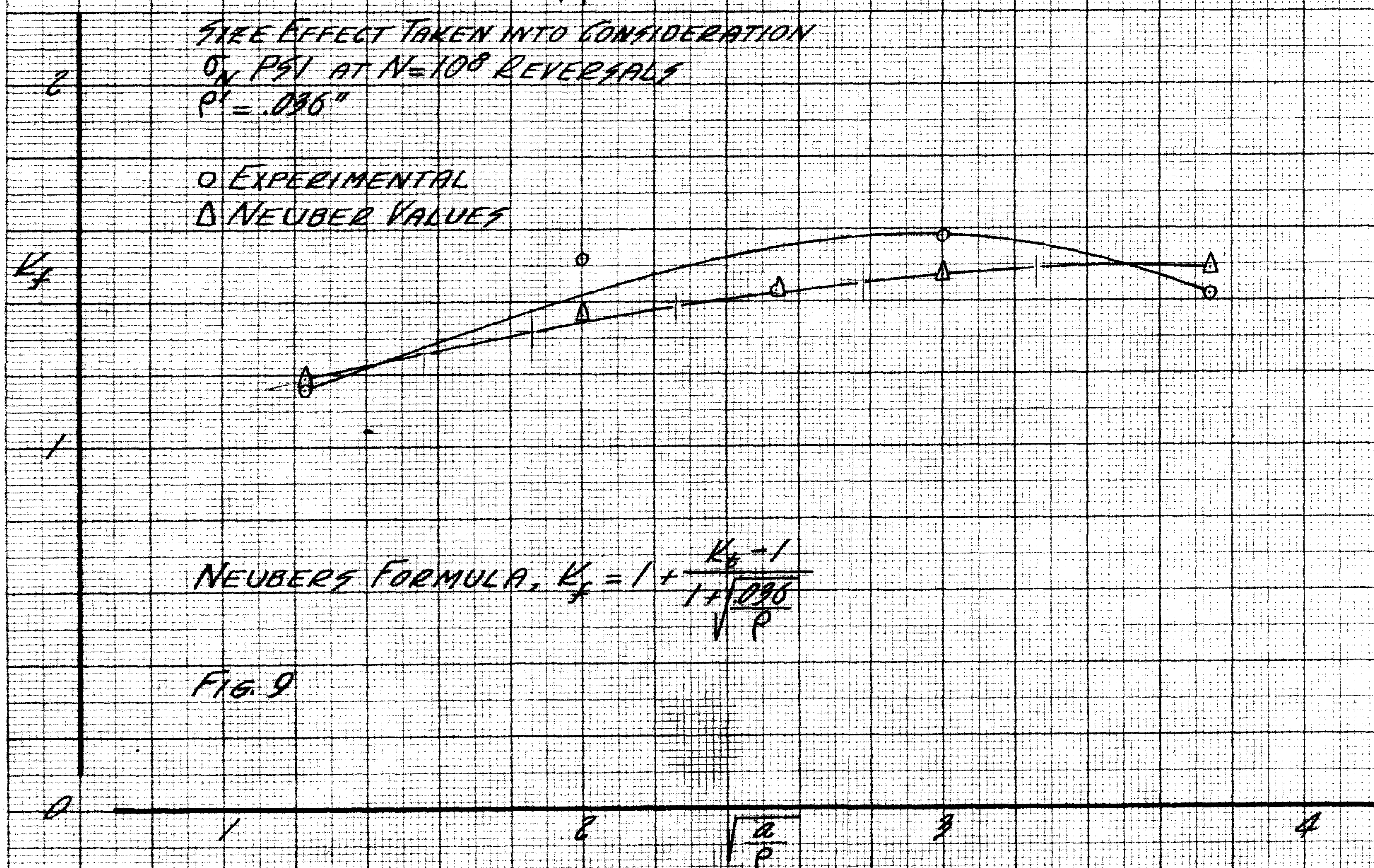

FIG. 9

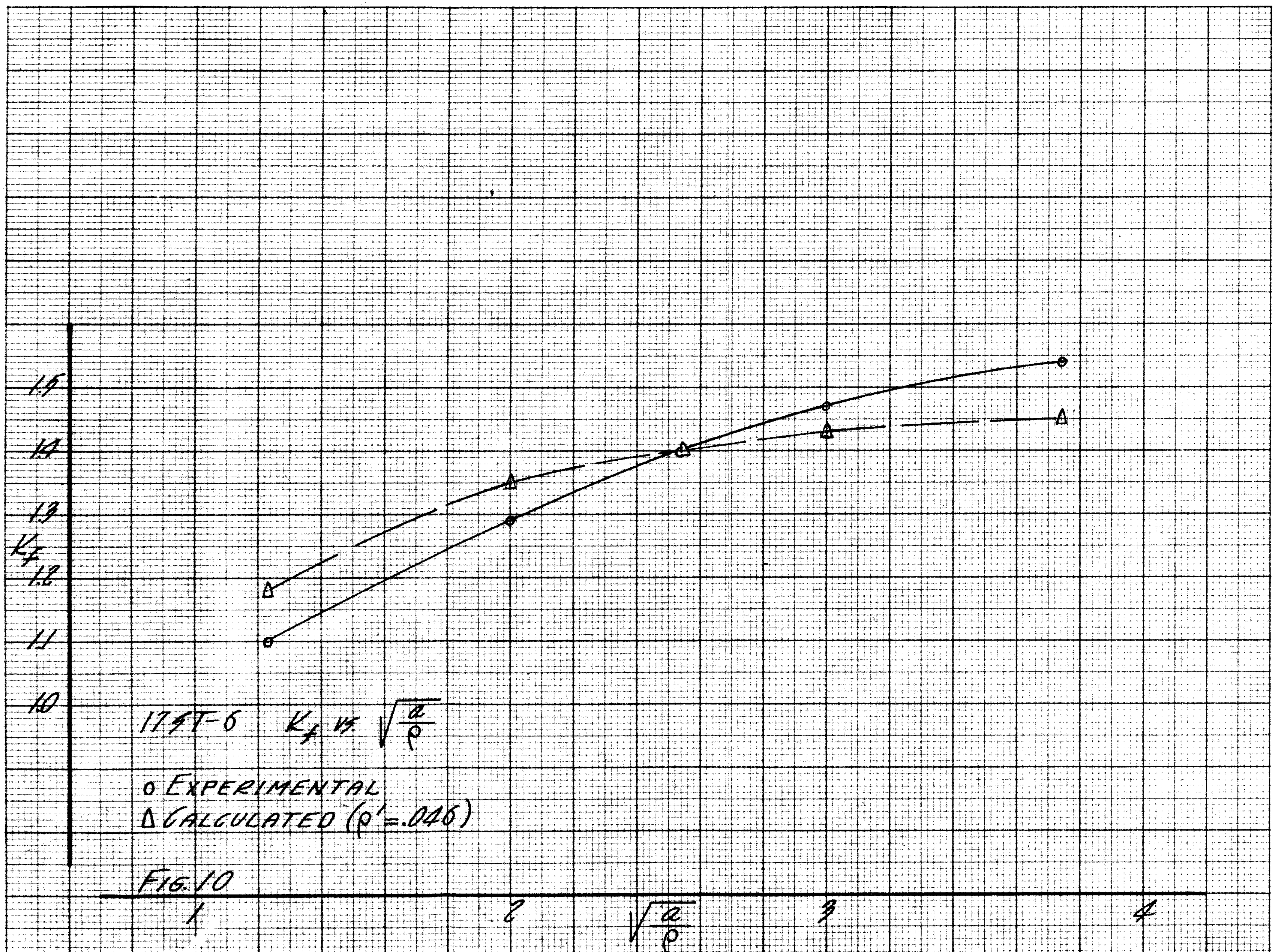

1.5
1.4
1.3
K_f
1.2
1.1
1.0
17ST-6 K_f vs. $\sqrt{\frac{a}{\rho}}$
o EXPERIMENTAL
Δ CALCULATED (ρ'=.046)
1
2
$\sqrt{\frac{a}{\rho}}$
3
4

FIG. 10

KEUFFEL & ESSER CO., N. Y. NO. 359-61
Semi-Logarithmic, 2 cycles × 10 to the inch, 5th lines accented.
MADE IN U. S. A.

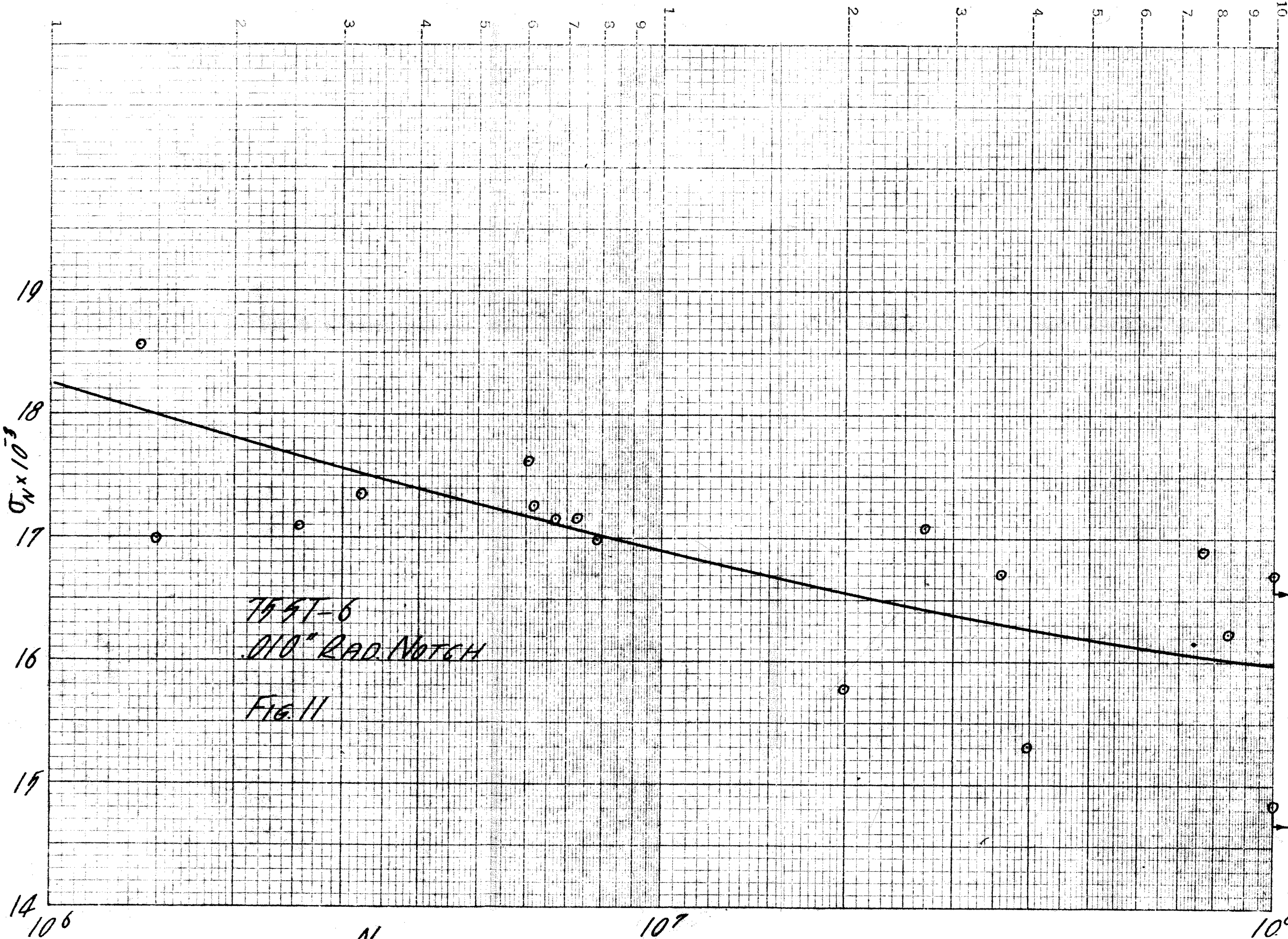

FIG. 11

KEUFFEL & ESSER CO., N. Y. NO. 359-61
Semi-Logarithmic 2 cycles × 10 to the inch, 5th lines accented
MADE IN U. S. A.

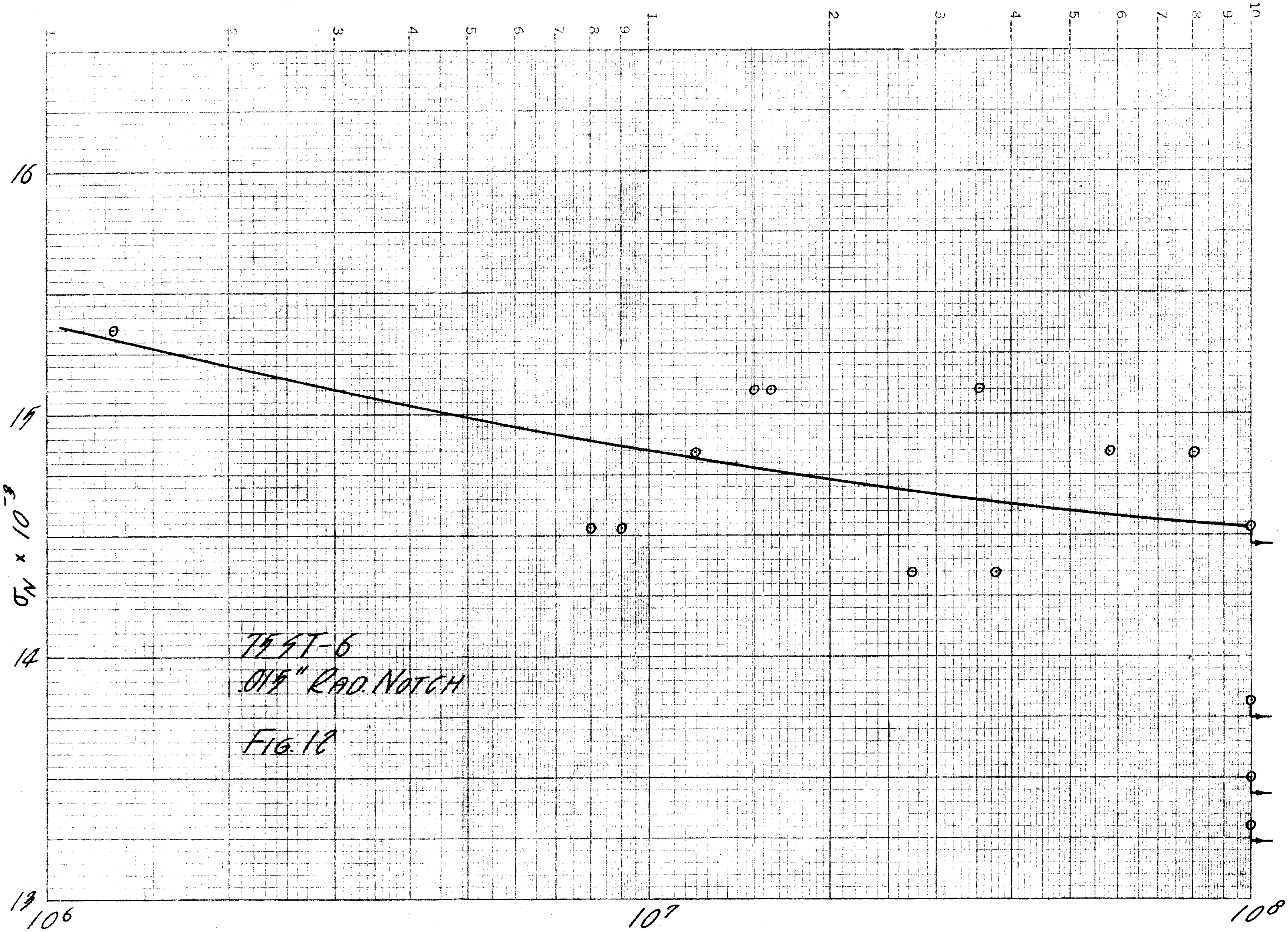

FIG. 12

359-61 KEUFFEL & ESSER CO.
Semi-Logarithmic. 2 Cycles × 10 to the inch.
5th lines accented.
MADE IN U.S.A.

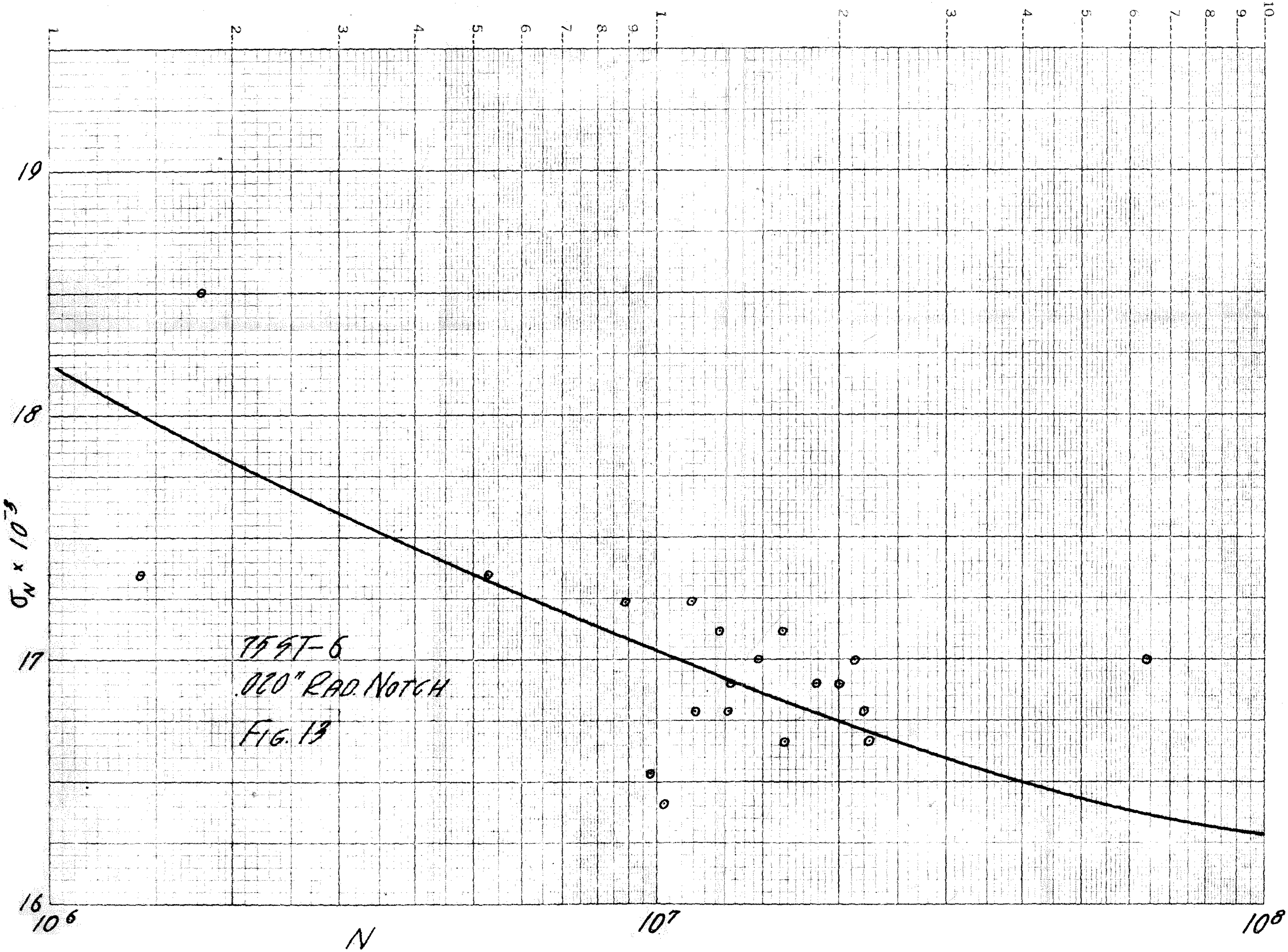

FIG. 13

KEUFFEL & ESSER CO., N. Y. NO. 359-51
Semi-Logarithmic, 2 cycles X 10 to the inch, 5th lines accented.
MADE IN U. S. A.

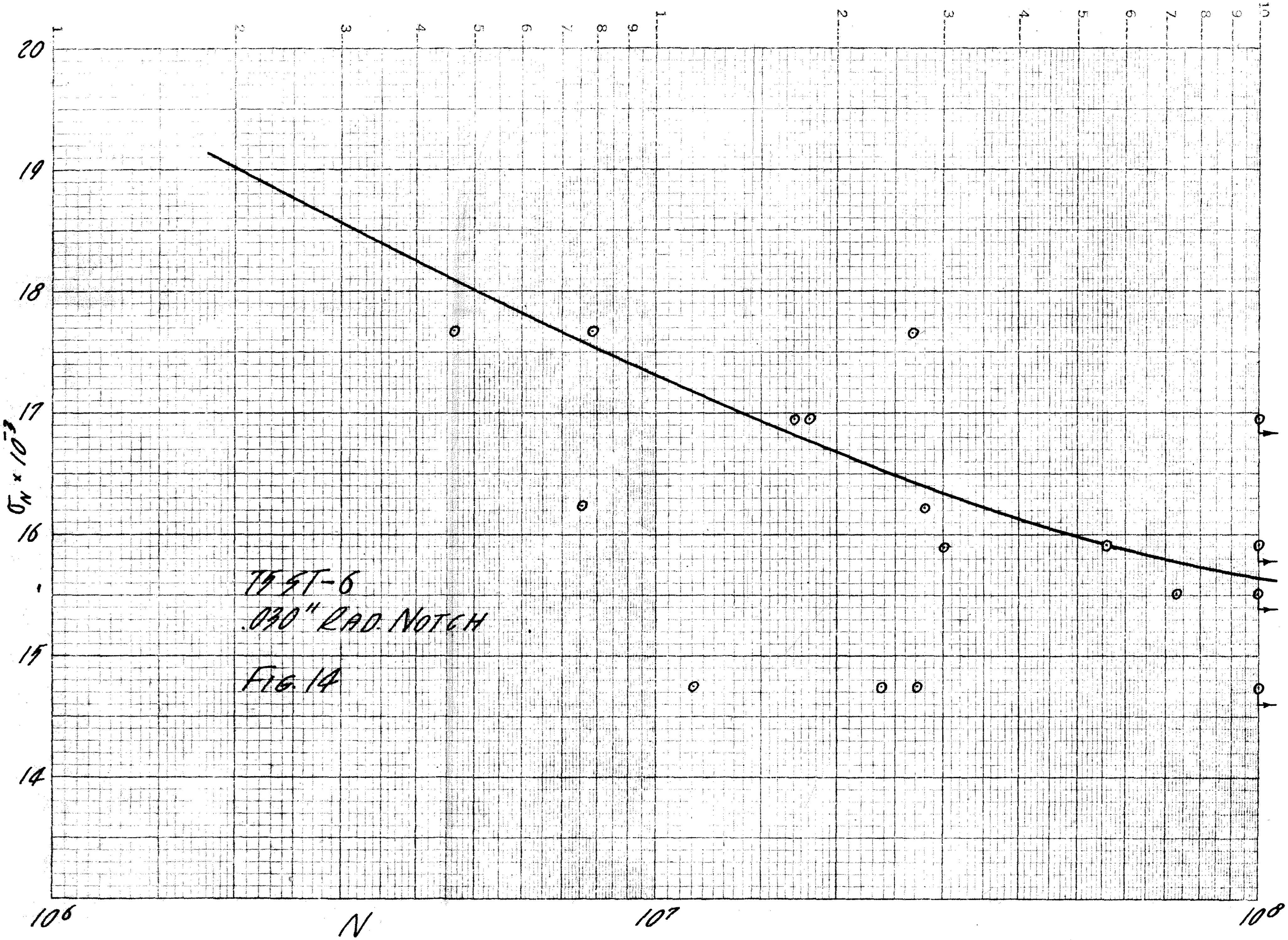

FIG. 14

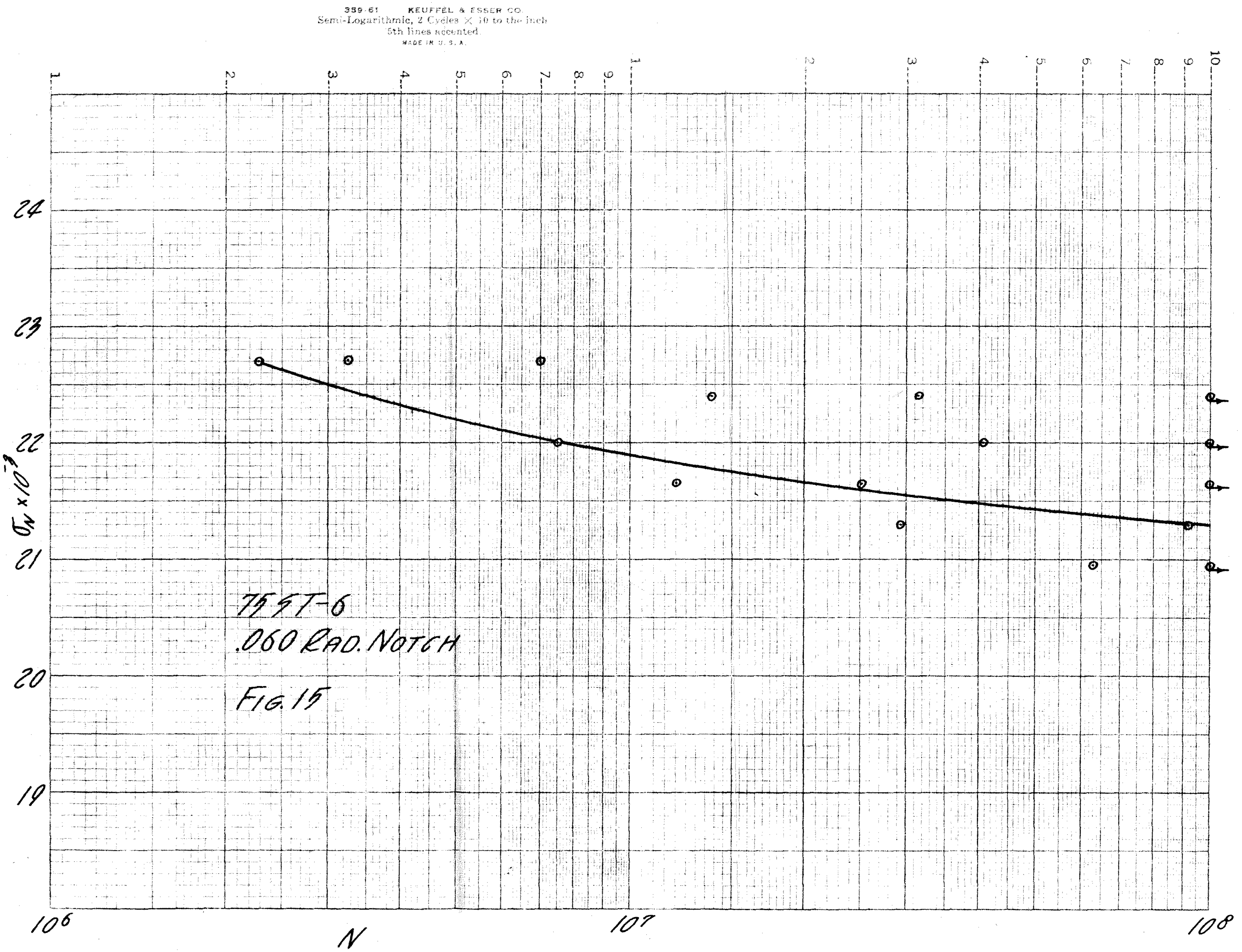
359-61 KEUFFEL & ESSER CO.
Semi-Logarithmic, 2 Cycles × 10 to the inch
5th lines accented
MADE IN U. S. A.
24
23
22
21
20
19
$\sigma_N \times 10^{-3}$
10^6
10^7
10^8
N
75ST-6
.060 RAD. NOTCH

FIG. 15

359-61 KEUFFEL & ESSER CO.
Semi-Logarithmic, 2 Cycles X 10 to the inch
5th lines accented.
MADE IN U.S.A.

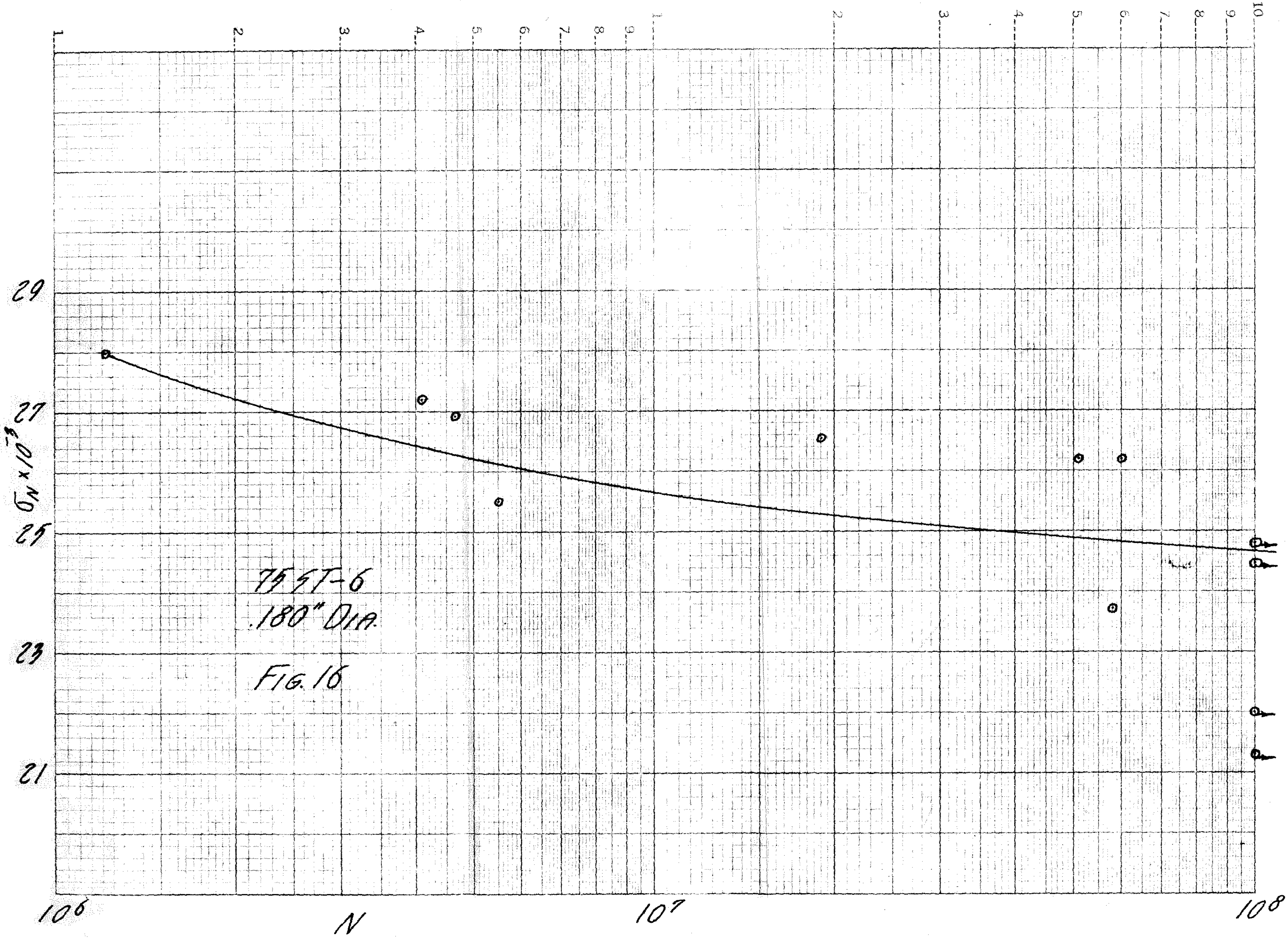

FIG. 16

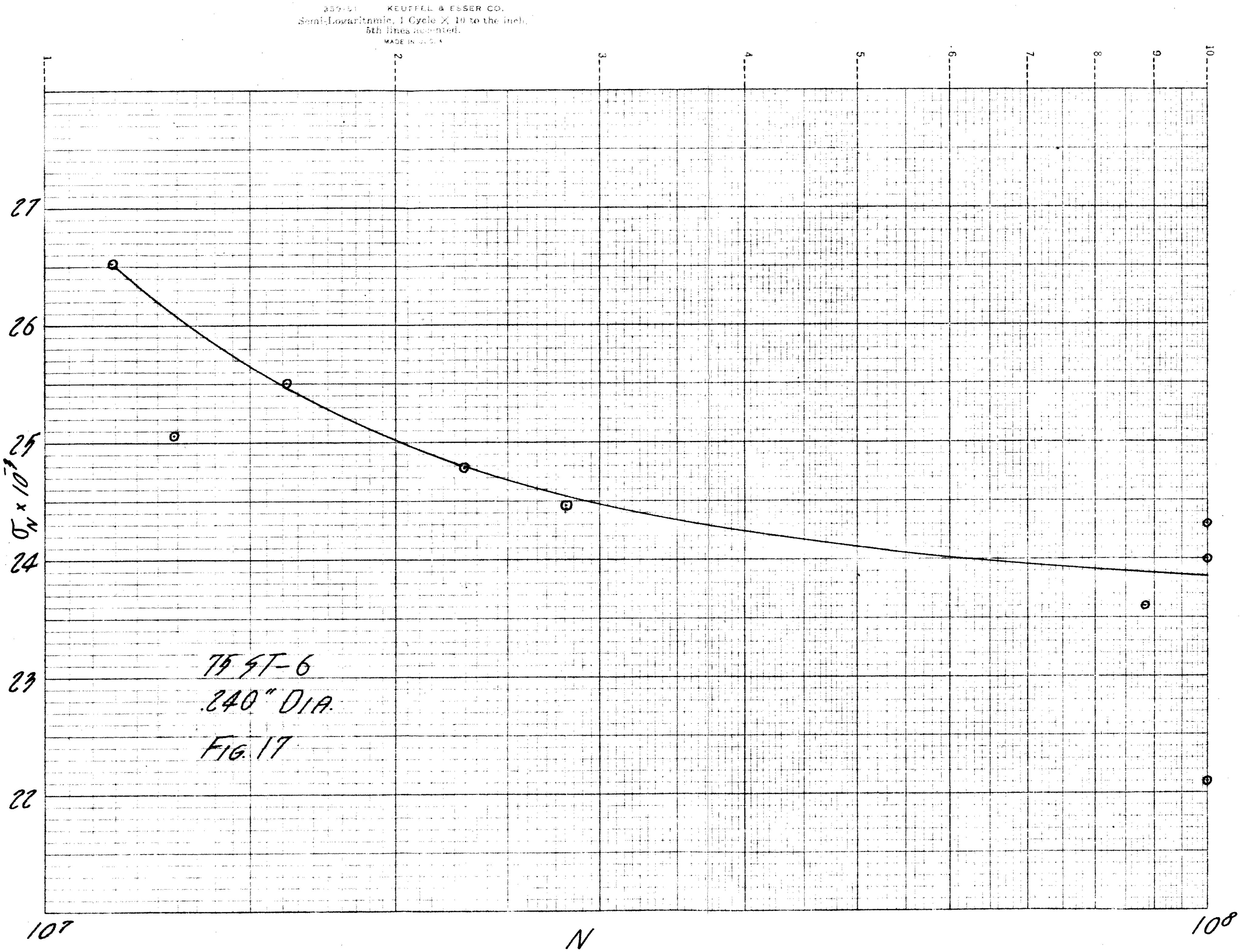
359-51 KEUFFEL & ESSER CO.
Semi-Logarithmic, 1 Cycle X 10 to the inch.
5th lines accented.
MADE IN U.S.A.
1
2
3
4
5
6
7
8
9
10
27
26
25
24
23
22
$\sigma_N \times 10^{-3}$
10^7
10^8
N
75 ST-6
.240" DIA.

FIG. 17


359-61 KEUFFEL & ESSER CO.
Semi-Logarithmic, 2 Cycles × 10 to the inch
5th lines accented.
MADE IN U.S.A.
27
26
25
24
23
22
$\sigma_N \times 10^{-3}$
75 ST-6
.280" DIA.
10^6
10^7
10^8
N

FIG. 18

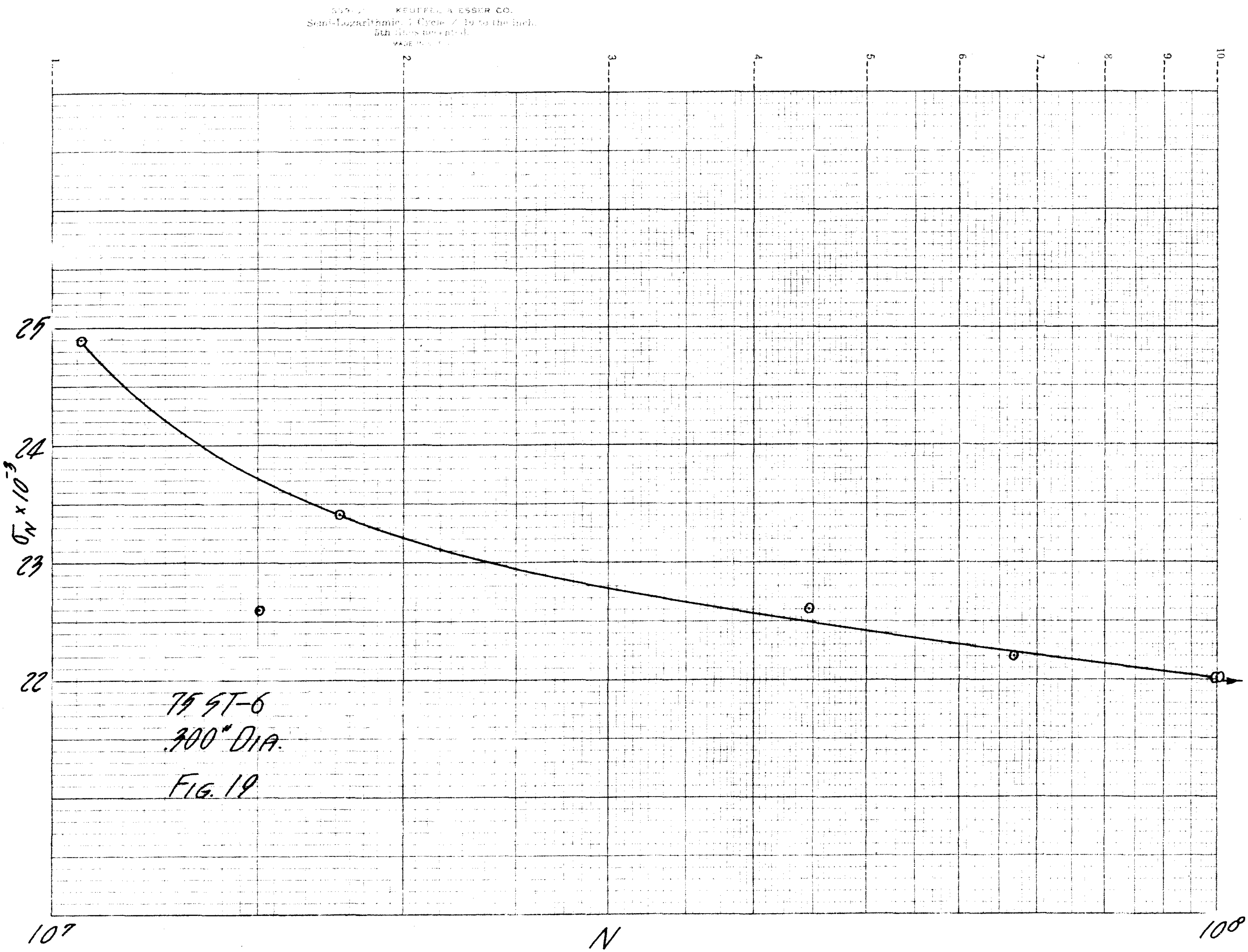
KEUFFEL & ESSER CO.
Semi-Logarithmic, 1 Cycle × 10 to the inch
5th lines accented
25
24
23
22
σN × 10⁻³
75 ST-6
.300" DIA.
10⁷
N
10⁸

FIG. 19

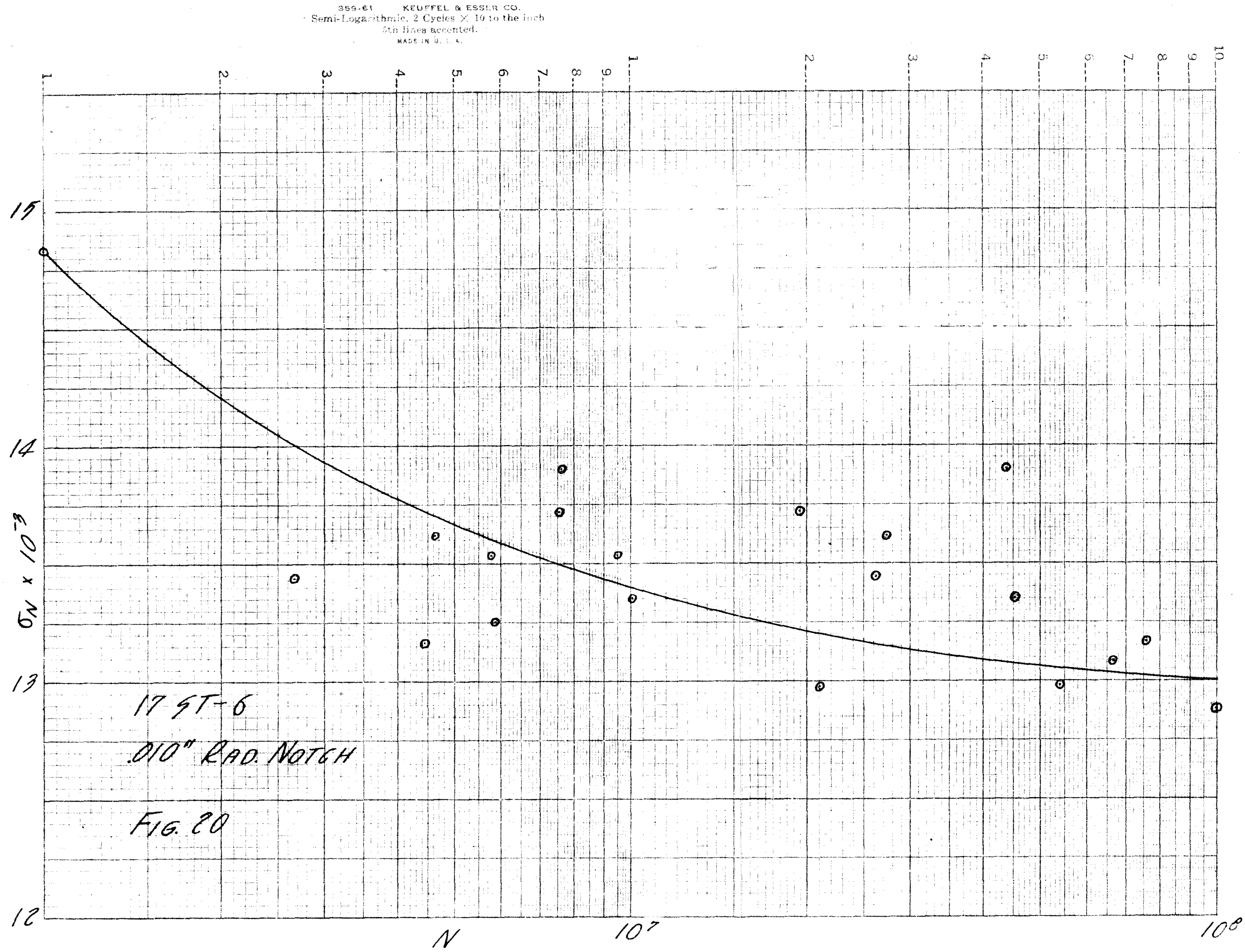

359-61 KEUFFEL & ESSER CO.
Semi-Logarithmic, 2 Cycles × 10 to the inch
5th lines accented.
MADE IN U. S. A.
15
14
13
12
σN x 10-3
N
10^7
10^8
17 ST-6
.010" RAD. NOTCH
FIG. 20

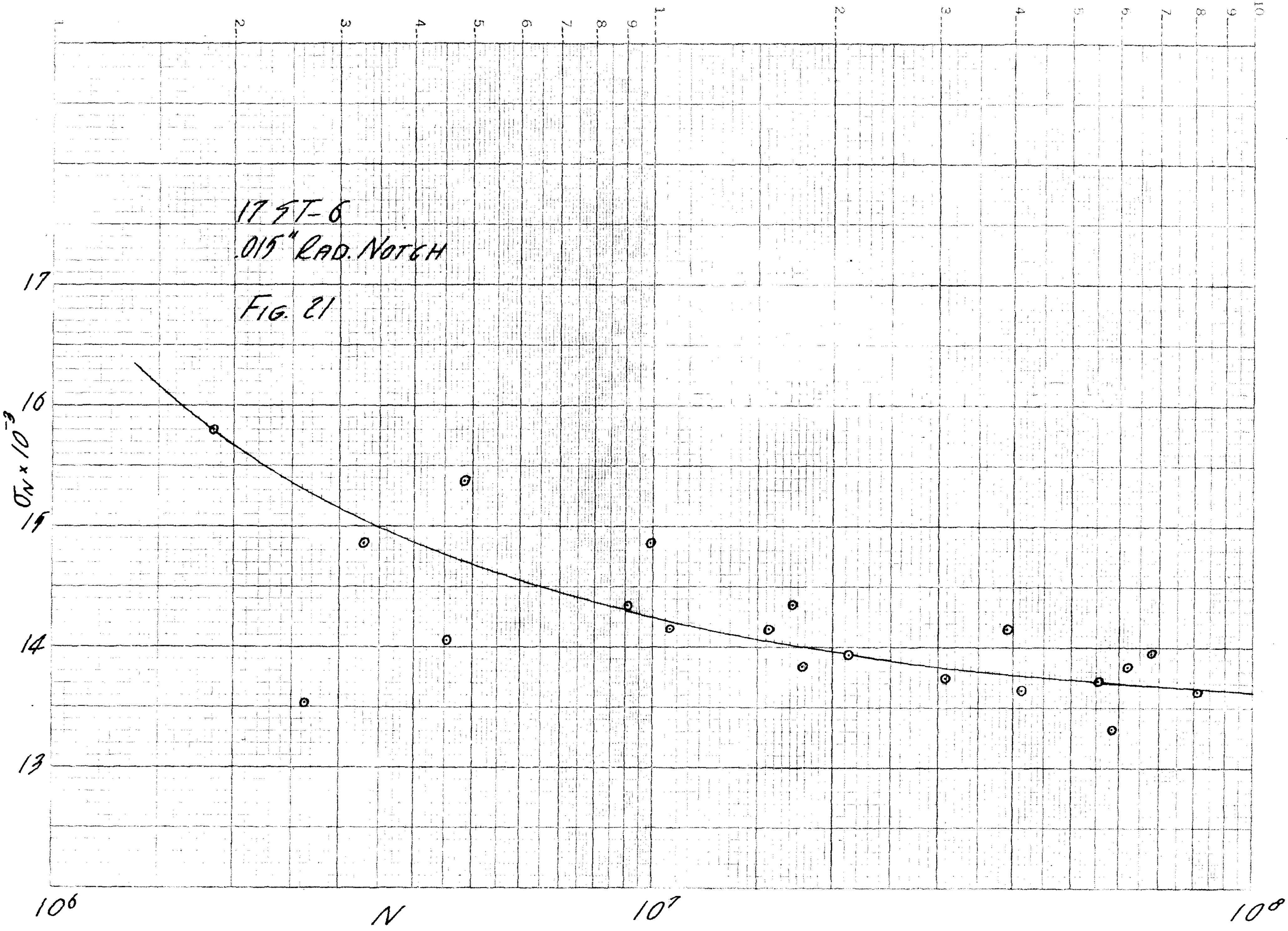
359-61 KEUFFEL & ESSER CO.
Semi-Logarithmic, 2 Cycles × 10 to the inch.
5th lines accented.
MADE IN U.S.A.
17 ST-6
.015" RAD. NOTCH
FIG. 21
17
16
15
14
13
$\sigma_N \times 10^{-3}$
10^6
N
10^7
10^8

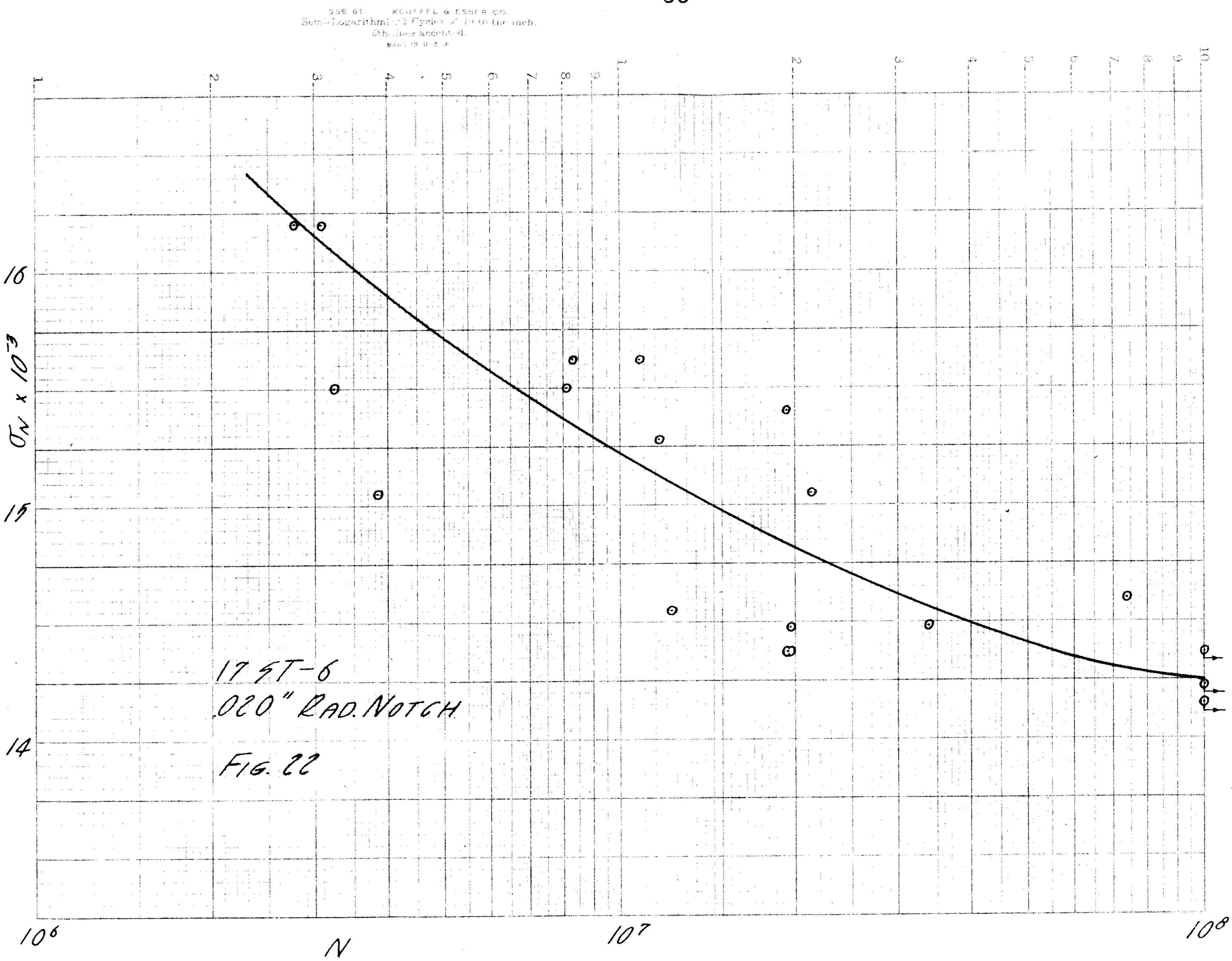
359-61 KEUFFEL & ESSER CO.
Semi-Logarithmic 2 Cycles × 10 to the inch.
5th lines accented.
MADE IN U.S.A.
16
15
14
$\sigma_N \times 10^3$
10^6
N
10^7
10^8
17 ST-6
.020" RAD. NOTCH
FIG. 22

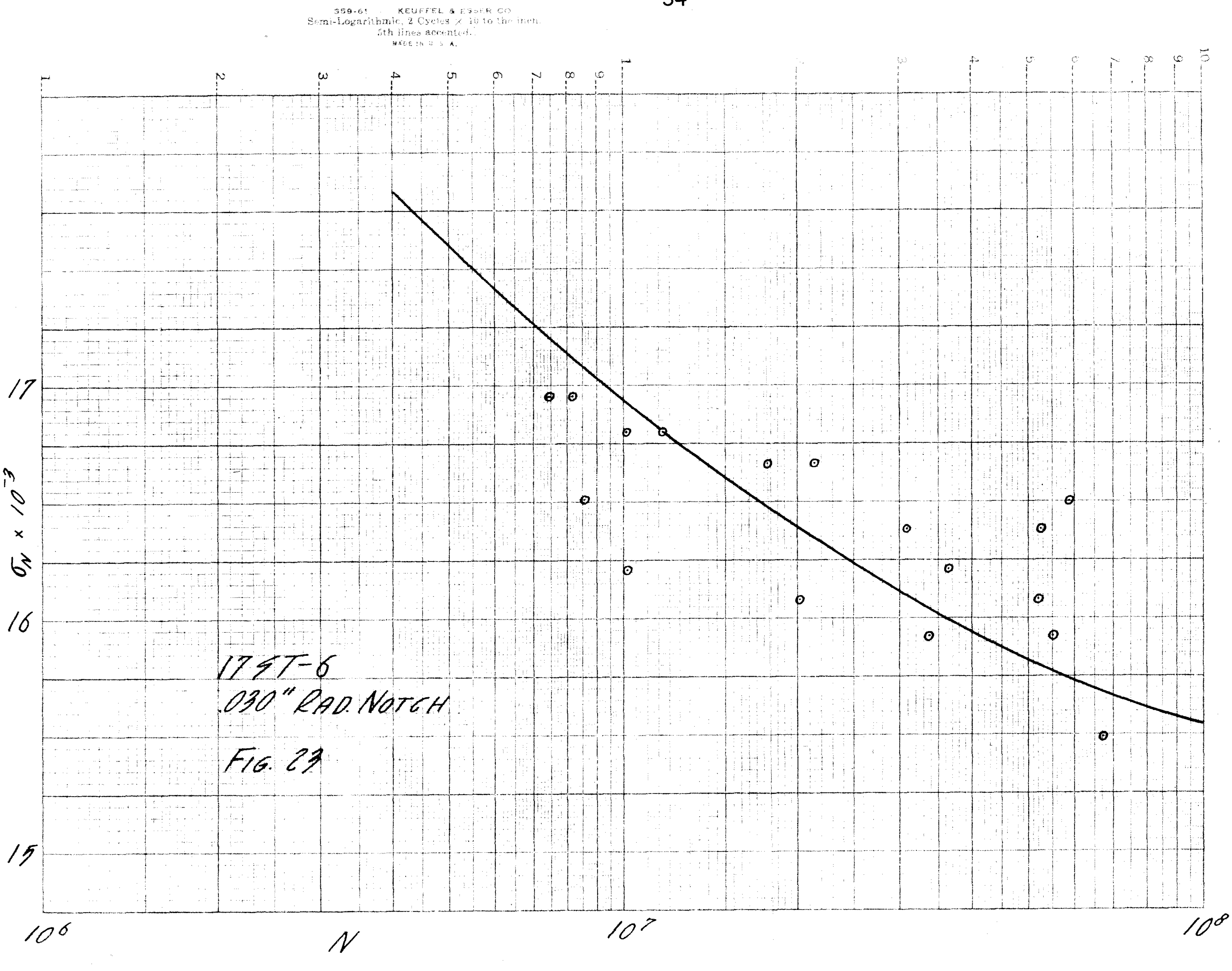
359-61 KEUFFEL & ESSER CO.
Semi-Logarithmic, 2 Cycles × 10 to the inch.
5th lines accented.
MADE IN U. S. A.
17
16
15
σN × 10⁻³
10⁶
N
10⁷
10⁸
17 ST-6
.030" RAD. NOTCH

FIG. 23

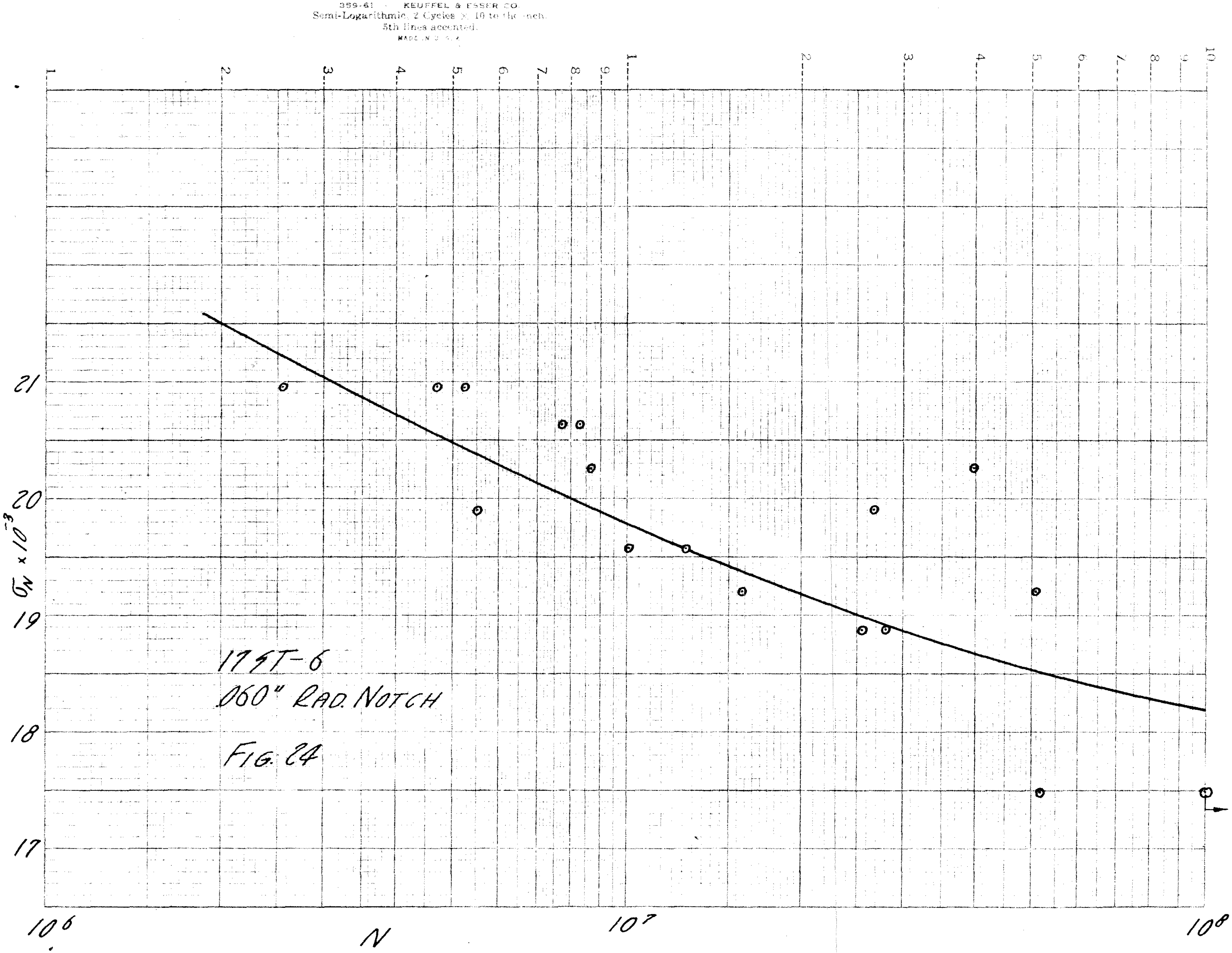
359-61 KEUFFEL & ESSER CO.
Semi-Logarithmic, 2 Cycles × 10 to the inch.
5th lines accented.
21
20
19
18
17
$\sigma_N \times 10^{-3}$
10^6
10^7
10^8
N
17ST-6
.060" RAD. NOTCH

FIG. 24

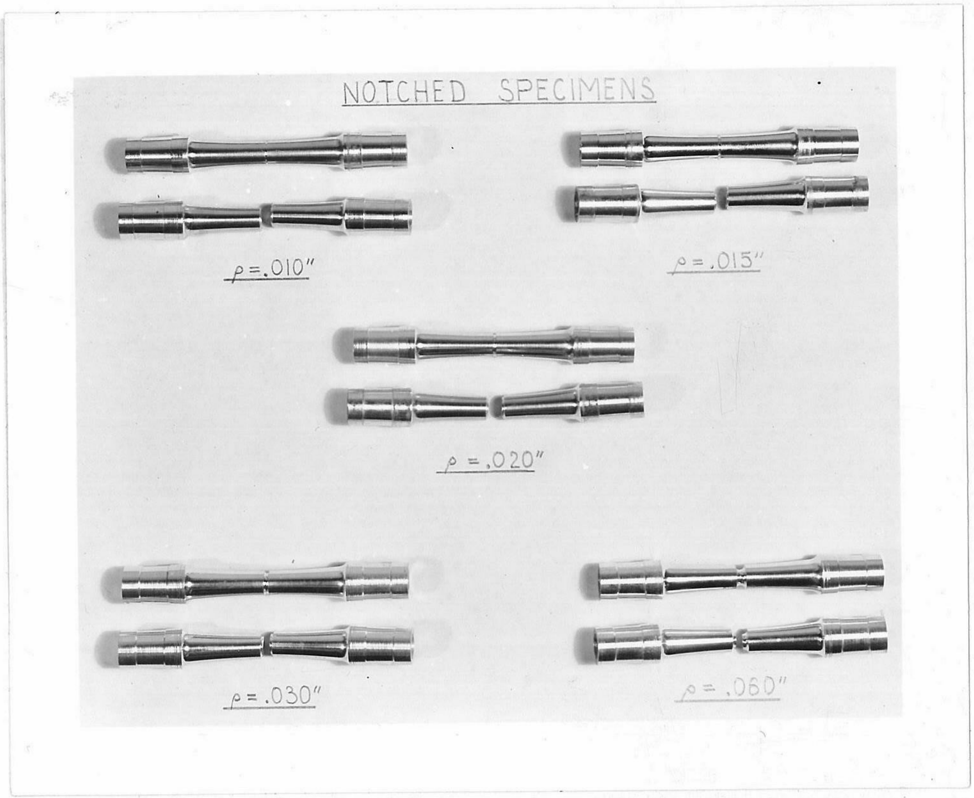

PLATE NO. 1

The notched specimens.

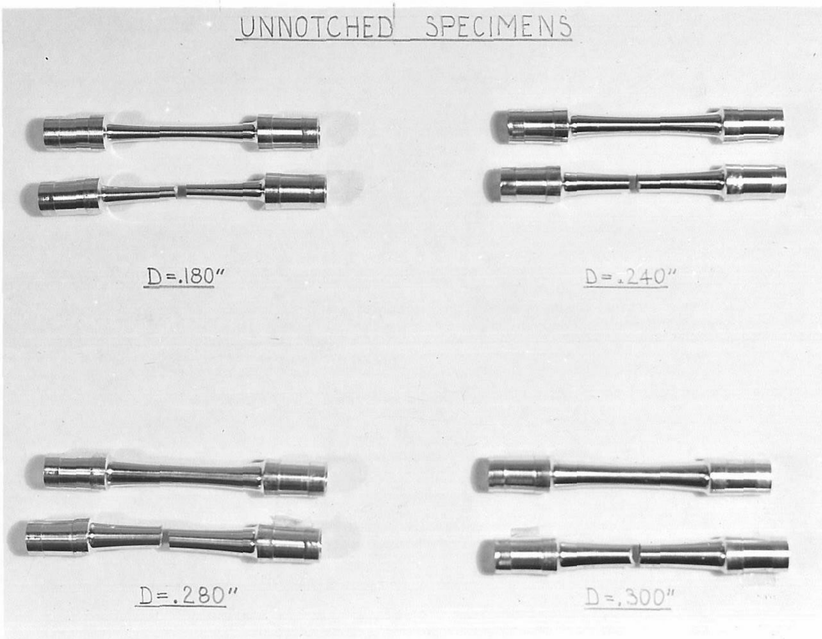

PLATE NO. 2

The unnotched specimens.

PLATE NO. 3

This is a typical fracture of a notched specimen. (Unnotched specimen identical.) The fractures were generally normal to the longitudinal axes of the specimen. The first crack starts at the surface of the specimen and spreads itself in crescent form (darker region up to a certain extent after which suddeh failure occurs (lighter region).

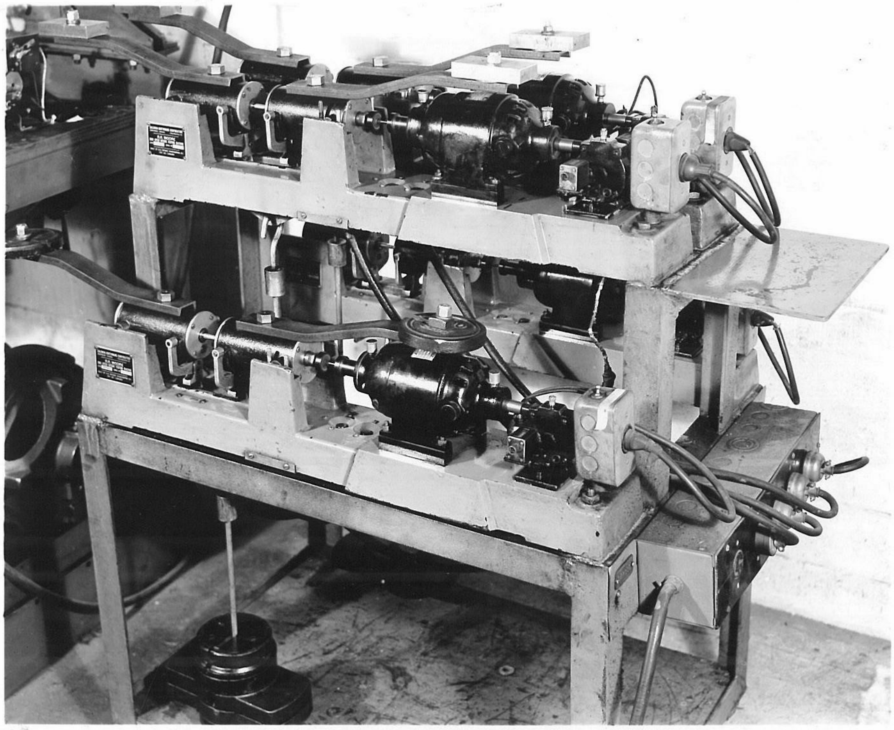

PLATE NO. 4

The standard R. R. Moore rotating beam fatigue machine. Note the counterweights attached to the bearing oil holes so as to have zero tare load.